Journal of Hydrology 538 (2016) 625–639

Contents lists available at ScienceDirect

Journal of Hydrology

journal homepage: www.elsevier.com/locate/jhydrol

Evaluating the variability in surface water reservoir planning characteristics during climate change impacts assessment

Bankaru-Swamy Soundharajan [a], Adebayo J. Adeloye [a,*], Renji Remesan [b]

[a] Institute for Infrastructure and Environment, Heriot-Watt University, Edinburgh EH14 4AS, United Kingdom
[b] Cranfield Water Science Institute, Cranfield University, Bedford, United Kingdom

ARTICLE INFO

Article history:
Received 27 January 2016
Accepted 25 April 2016
Available online 30 April 2016
This manuscript was handled by Andras Bardossy, Editor-in-Chief, with the assistance of Sheng Yue, Associate Editor

Keywords:
Reservoir performance
Climate change
Uncertainty analysis
Pong reservoir
India

SUMMARY

This study employed a Monte-Carlo simulation approach to characterise the uncertainties in climate change induced variations in storage requirements and performance (reliability (time- and volume-based), resilience, vulnerability and sustainability) of surface water reservoirs. Using a calibrated rainfall–runoff (R–R) model, the baseline runoff scenario was first simulated. The R–R inputs (rainfall and temperature) were then perturbed using plausible delta-changes to produce simulated climate change runoff scenarios. Stochastic models of the runoff were developed and used to generate ensembles of both the current and climate-change-perturbed future runoff scenarios. The resulting runoff ensembles were used to force simulation models of the behaviour of the reservoir to produce 'populations' of required reservoir storage capacity to meet demands, and the performance. Comparing these parameters between the current and the perturbed provided the population of climate change effects which was then analysed to determine the variability in the impacts. The methodology was applied to the Pong reservoir on the Beas River in northern India. The reservoir serves irrigation and hydropower needs and the hydrology of the catchment is highly influenced by Himalayan seasonal snow and glaciers, and Monsoon rainfall, both of which are predicted to change due to climate change. The results show that required reservoir capacity is highly variable with a coefficient of variation (CV) as high as 0.3 as the future climate becomes drier. Of the performance indices, the vulnerability recorded the highest variability (CV up to 0.5) while the volume-based reliability was the least variable. Such variabilities or uncertainties will, no doubt, complicate the development of climate change adaptation measures; however, knowledge of their sheer magnitudes as obtained in this study will help in the formulation of appropriate policy and technical interventions for sustaining and possibly enhancing water security for irrigation and other uses served by Pong reservoir.

1. Introduction

Climate change is predicted to affect the hydrology of most regions through its influence on temperature, rainfall, evapotranspiration (IPCC, 2007) and ultimately the runoff, the planning characteristics (e.g. capacity) and the performance (reliability, resilience, vulnerability and sustainability) of water resources infrastructures such as reservoirs. These impacts must be quantified for better planning and operation of water resource systems. Several studies have investigated the effects of climate change on reservoirs including Fowler et al. (2003), Nawaz and Adeloye (2006), Burn and Simonovic (1996), Li et al. (2009) and Lopez et al. (2009), with majority of these predicting worsening reservoir performance and higher storage capacity requirements as a consequence of climatic change. Relatively more recently, Raje and Mujumdar (2010) investigated the effect of hydrological uncertainty of climate change predictions on the performance of the Hirakud reservoir on the Mahanadi River in Orissa, India and found worsening reliability and vulnerability situations in the future.

A common feature of published studies is that they have forced the impacts models with outputs of large scale GCMs that have been downscaled to the catchment scale using either the statistical or dynamical (i.e. regional climate models) downscaling protocols. Fowler et al. (2007) discuss the pros and cons of these two approaches but despite their popularity for water resources climate change impact studies, there still remains a lot of uncertainties in both the broad-scale GCM predictions and their corresponding catchment scale downscaled hydro-climatology as noted by Raje and Mujumdar (2010). Adeloye et al. (2013) discuss

* Corresponding author.
E-mail address: a.j.adeloye@hw.ac.uk (A.J. Adeloye).

http://dx.doi.org/10.1016/j.jhydrol.2016.04.051
0022-1694/

the nature of these uncertainties and the problems they pose for decision makers trying to develop adaptation measures for projected climate change impacts. Peel et al. (2014) distinguish between-GCMs and within-GCM uncertainties, the latter relating to the inability of a GCM to produce the same output over different runs, while the former concerns variability in outputs of different GCM experiments caused largely by structural, parameterisation and initialisation differences. To avoid the complications and uncertainties in downscaled GCM climate predictions, change factor (delta perturbation) method is suggested (Anandhi et al., 2011; Vicuna et al., 2012), in which plausible changes in the runoff impacting weather variables such as precipitation and temperature are assumed and the effect of these on runoff is simulated using a suitable hydrological model.

However, whether based on downscaled GCMs or delta perturbations, the traditional approach that uses single traces of both the current and future hydrology fails to recognise that these single traces represent one realisation of the population of possible traces. Thus, any impact estimated using the single traces can only relate to the average impact; no information is available on either the possible range of impacts or the variability (or uncertainties) of the assessed impacts. To be able to provide these answers, the population (or ensemble) of the current and future climate is required. Peel et al. (2014) did this to characterise the within-GCM variability by replicating (100 times) GCM-based runs of current and future climate. These were then used to force a hydrological model, leading ultimately to the evaluation of uncertainties and variability in runoff and reservoir yields.

The work reported here has characterised the uncertainties in climate change impacts on the planning characteristics of surface water reservoirs using an approach similar to that described by Peel et al. (2014). However, major differences between the current study and Peel et al. (2014) include that: delta perturbations instead of downscaled GCM climate change scenarios are used; stochastic modelling is used to derive replicates of runoff series directly, rather than the indirect approach by Peel et al. (2014) in which the rainfall and temperature were modelled stochastically and later used to force a rainfall–runoff model, thus removing the added layer of uncertainty caused by the multi-ensemble rainfall–runoff modelling; and reservoir impacts analysis is not limited to the yield/storage alone but includes consideration of performance indices. As far as the authors are aware, this is the first attempt at characterising the variability of reservoir performance indices within the context of climate change impacts assessment.

To demonstrate the applicability of the methodology, it was applied to the Pong reservoir located on the Beas River in Himachal Pradesh, India (see Fig. 1). The Pong reservoir principally provides irrigation water although, prior to its diversion to irrigation, its released water first passes through turbines for generating electricity (Jain et al., 2007). Consequently, the current study is focusing on the irrigation function of the reservoir. The reservoir inflow is highly influenced by both the Monsoon rainfall and the melting glacier and seasonal snow from the Himalayas; consequently, its ability to satisfactorily perform its functions is susceptible to possible climate-change disturbances in these climatic attributes. For a system that is inextricably linked to the socio-economic well-being of its region (Jain et al., 2007), any significant deterioration in performance or ability to meet the irrigation water demand will have far reaching consequences. This is why it is important to carry out a systematic assessment of the performance of the reservoir during climate change and to use the outcome to potentially inform the development of appropriate solutions.

In the following sections, more details about the adopted methodology are given. These are then followed by the case study after which the results are presented and discussed. The final section contains the conclusions.

2. Methodology

The flowchart of the methodology is shown in Fig. 2.

2.1. HYSIM hydrological model

HYSIM was used to simulate catchment runoff in the study. HYSIM is a time-continuous, conceptual rainfall–runoff model. The model has two sub-routines simulating, respectively, river basin hydrology and the channel hydraulics. The hydrology is simulated with help of seven stores representative of land use and soil type while the hydraulic sub-routine is conducted using kinematic routing of flows. The full structure of the model is schematically illustrated in Fig. 3.

The seven natural stores into which the hydrology routine was conceptualised comprise interception storage, upper soil horizon, lower soil horizon, transitional groundwater store, groundwater store, snow storage and minor channel storage, all with associated hydrological parameters as detailed by Pilling and Jones (1999). The interception storage in the model denotes canopy storage of moisture and is determined by the vegetation type in the model. Water stored in the interception compartment is ultimately lost by evaporation. The transitional groundwater store is conceptualised as an infinite linear reservoir, and serves to represent the first stage of groundwater storage. The store receives water from both the upper and lower soil horizons through the process of deep percolation when these horizons are at or above the field capacity. Water in the transitional groundwater store is constantly discharging to the permanent groundwater store also through deep percolation.

Initial values of some of the panoply of model parameters (see Pilling and Jones, 1999) are usually estimated from land use and soil type of the region while others are often extracted from the literature. Some of these parameters are later refined by calibration including: rooting depth (mm) [RD], permeability – horizon boundary (mm/h) [PHB], permeability – base lower horizon (mm/h) [PBLH], interflow – upper (mm/h) [IU], interflow – lower (mm/h) [IL], snow threshold [ST], and snow melt rate (mm/°C) [SM]. RD depends on the type of vegetation but usually ranges between 800 mm and 5000 mm, with lower value associated with grassland and higher value for woodland. For other parameters like PHB, PBLH, IU and IL, a universal default initial value of 10 mm/h is assumed in the model. The snow melt related parameters, i.e. ST and SM control respectively the temperature below which the precipitation falls as snow and the melt rate in mm for each degree of temperature above the threshold.

The hydraulics routine routes the flow down the channel using a simple kinematic wave approach, also with associated parameters (Manley and WRA, 2006). As will be shown later, the Beas at the Pong catchment was modelled as three sub-catchments in series to account for the spatial variability in the catchment. The relevant channel hydraulics parameters for the three sub-basins in the Beas basin are shown in Table 1. None of these were optimised during the runs carried out in this study.

HYSIM takes precipitation, temperature and, where available, the potential evaporation as inputs. The temperature is required for the modelling of snow-melt and accumulation based on the empirical degree-day approach. Where estimates of the potential evaporation are unavailable *a priori*, the temperature is also utilised for estimating the evapotranspiration. HYSIM has been extensively used in several research studies including snowy catchments of the United Kingdom to address climate change impacts issues e.g. Pilling and Jones (1999, 2002), Arnell (2003), Wilby (2005). Murphy et al. (2006) used HYSIM for hydrological simulations associated with climate change water resources impacts studies

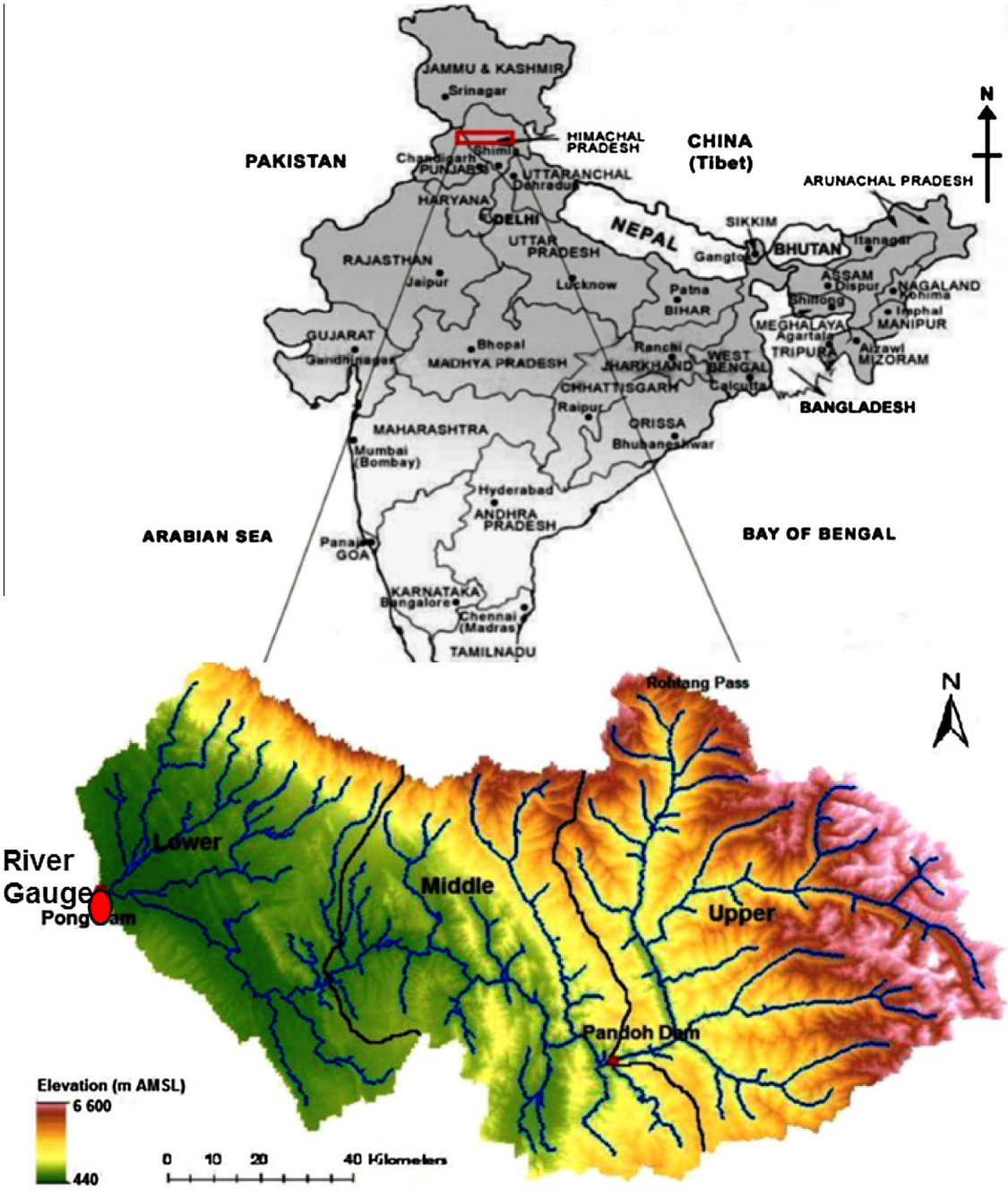

Fig. 1. Beas River basin.

in Ireland using downscaled data from the output from the HadCM3 global circulation model with satisfactory results.

2.2. Stochastic data generation for Monte Carlo simulation

The Monte Carlo simulation relies on generating several realisations of the at-site reservoir inflow runoff data. In the case study application, 1000 such replicates were generated. Prior to the generation, two issues must be settled: the temporal scale and the form of the stochastic generation model to use. Regarding the former, the decision was made to restrict the analysis to the monthly time scale. As noted by Adeloye (2012), the monthly time scale is sufficient for reservoir planning analysis as it will cater for both the within-year and over-year storage requirements. This implies that monthly data must be generated using an appropriate stochastic model.

The generation of monthly data can be achieved using one of two approaches: either generating annual runoff data and disaggregating these to monthly values using an appropriate disaggregation scheme (e.g. method of fragments (Svanidze, 1964; Srikanthan and McMahon, 1982); method of pro-ration (Savic et al., 1989); the Valecia–Schaake disaggregation (Valencia and Schaake, 1973)) or by utilizing a monthly generation model such as the Thomas–Fiering generation model (Thomas and Fiering, 1962) to directly generate the monthly data. Given the between-disaggregation scheme variability of disaggregated runoff and the consequent non-uniqueness of the outcome of reservoir planning analyses (see Silva and Portela, 2012), a monthly runoff generation

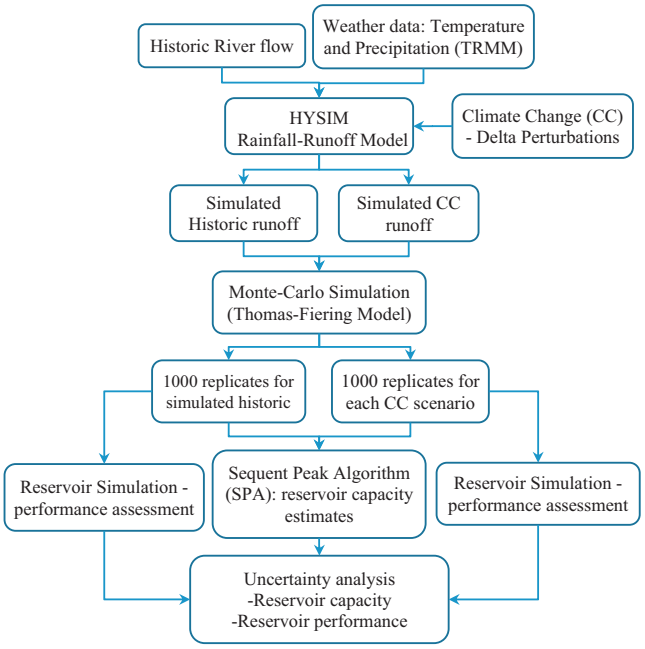

Fig. 2. Methodology flow chart.

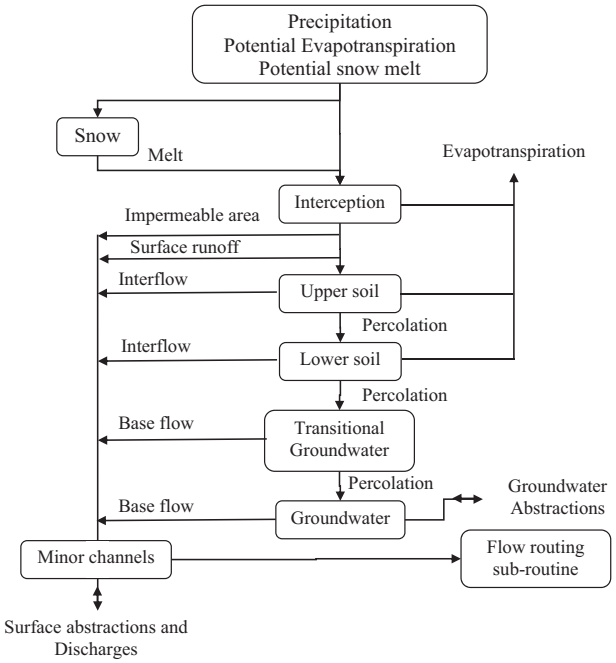

Fig. 3. HYSIM schematic.

Table 1
HYSIM hydraulic parameters.

Parameters	Sub-basin		
	Upper	Middle	Lower
Channel roughness	0.03	0.03	0.03
Reach gradient	0.035	0.007	0.0025
Flood plain roughness	0.10	0.10	0.10

model was used. Thus, replicates of monthly runoff were simulated using the Thomas–Fiering monthly model (McMahon and Mein, 1986):

$$\left.\begin{aligned} Q_2 &= \mu_{Feb} + b_{Feb/Jan}(Q_1 - \mu_{Feb}) + t_n\sigma_{Feb}\sqrt{(1-\rho^2_{Feb/Jan})} \\ &\vdots \\ Q_{13} &= \mu_{Jan} + b_{Jan/Dec}(Q_{12} - \mu_{Jan}) + t_n\sigma_{Jan}\sqrt{(1-\rho^2_{Jan/Dec})} \end{aligned}\right\} \quad (1)$$

$$b_{Feb/Jan} = \rho_{Feb/Jan}\frac{\sigma_{Feb}}{\sigma_{Jan}} \quad (2)$$

where Q_1, Q_2 are generated flows for month January and February respectively; μ is mean flow for the month indicated; b is least square regression coefficient (Eq. (2)); t_n is normal random variate with zero mean and unit variance; σ is standard deviation of flow for the month indicated; ρ is correlation coefficient between adjacent months as indicated. Eq. (1) assumes that monthly runoff is normally distributed, which may not be true. To remove the possible constraint that can be imposed by the normality assumption, the Box–Cox transformation (see Eq. (3)) was used to normalise the data:

$$Q' = \begin{cases} \frac{Q^{\lambda}-1}{\lambda}, & \lambda \neq 0 \\ \ln Q, & \lambda = 0 \end{cases} \quad (3)$$

where Q and Q' are untransformed (UT) and transformed (Tr) flows respectively, and λ is a parameter estimated such that the skewness of Q' becomes zero (McMahon and Adeloye, 2005).

After transformation using Eq. (3), the parameters (μ, σ, ρ) in Eqs. (1) and (2) are estimated based on the transformed data and are then used in Eq. (1) for the data generation. McMahon and Adeloye (2005) provide expressions for unbiased estimates of these and other parameters. The final step in the data generation is to bring back the generated values to the original values by applying the inverse of the Box–Cox transformation:

$$Q = (Q'\lambda + 1)^{1/\lambda} \quad (4)$$

2.3. Sequent peak algorithm (SPA) for capacity estimation

The first impact investigated is on the required capacity to meet existing demands at the Pong without failure when fed with the different runoff scenarios. A simple technique for obtaining the failure-free capacity estimate is the graphical mass curve (Ripple, 1883) but its graphical implementation makes the technique inconvenient especially for repeated analyses required for the Monte Carlo simulation. On the other hand, behaviour simulation is not efficient for failure-free capacity estimation because it is iterative, its outcome is not unique (see Adeloye et al., 2001) and has been found to mis-behave as demonstrated by Pretto et al. (1997). Thus, the required failure-free reservoir capacity was estimated using the sequent peak algorithm (SPA) which does not suffer from the above limitations (McMahon and Adeloye, 2005):

$$K_{t+1} = max(0, K_t + D_t - Q_t); \quad t \in N \quad (5)$$

$$K_a = max(K_{t+1}) \quad (6)$$

where K_a is reservoir capacity, K_{t+1} and K_t are respectively the sequential deficits at the end and start of time period t, D_t is the demand during t, Q_t is the inflow during t and N is the number of months in the data record. The SPA is a critical period reservoir sizing technique and like all such techniques assumes that the reservoir is full at start and end of the cycle, i.e. $K_0 = K_N = 0$. If, however, this is untrue, i.e. $K_N \neq 0$, the SPA cycle is repeated by setting the initial deficit to K_N, i.e. $K_0 = K_N$. This second iteration should end with K_N unless the demand is unrealistic, e.g. such as attempting to take a demand higher than the mean annual runoff from the reservoir. In this sense, the assumption of an initially full reservoir is not crucial for the SPA because if this assumption is not valid, it will

become evident at the end of the first cycle and a correction made for it during the second cycle.

2.4. Reservoir behaviour simulation and performance indices

To assess the performance of the historic reservoir capacity and operational rule curves when fed with the different runoff scenarios, behaviour simulation was carried out using (McMahon and Adeloye, 2005):

$$S_{t+1} = S_t + Q_t - D'_t; \quad LRC \leqslant S_{t+1} \leqslant URC \tag{7}$$

where S_{t+1}, S_t are respectively, reservoir storage at the end and beginning of time period t; D_t' is the actual water released during t (which may be different from the demand D_t, depending on the operating rule curves); LRC is the lower rule curve ordinate for the month corresponding to t; and URC is the corresponding upper rule curve ordinate.

Following simulation, relevant performance measures – reliability, vulnerability, resilience and sustainability – were evaluated as outlined below (see also McMahon and Adeloye, 2005; McMahon et al., 2006):

i. *Time-based Reliability* (R_t) is the proportion of the total time period under consideration during which a reservoir is able to meet the full demand without any shortages:

$$R_t = N_s/N \tag{8}$$

where N_s is the total number of intervals out of N that the demand was met.

ii. *Volume-based Reliability* (R_v) is the total quantity of water actually supplied divided by the total quantity of water demanded during the entire operational period:

$$R_v = \sum_{t=1}^{N} D'_t \Big/ \sum_{t=1}^{N} D_t, \quad \forall\ D'_t \leqslant D_t \tag{9}$$

iii. *Resilience* (φ) is a measure of the reservoir's ability to recover from failure (Hashimoto et al., 1982):

$$\varphi = 1 \Big/ \left(\frac{f_d}{f_s}\right) = \frac{f_s}{f_d}; \quad 0 < \varphi \leqslant 1 \tag{10}$$

where f_s is number of continuous sequences of failure periods and f_d is the total duration of the failures, i.e. $f_d = N - N_s$.

iv. *Vulnerability* (η) is the average period shortfall as a ratio of the average period demand (Sandoval-Soils et al., 2011):

$$\eta = \frac{\sum_{t=1}^{f_d}[(D_t - D'_t)/D_t]}{f_d}; \quad t \in f_d \tag{11}$$

v. *Sustainability index* integrates the three earlier defined indices (Sandoval-Soils et al., 2011):

$$\gamma_1 = (R_t \varphi (1-\eta))^{1/3} \tag{12}$$

where γ_1 is the sustainability. Because the volumetric reliability (R_v) is more robust than R_t, i.e. less likely to be dramatically affected, an alternative definition of sustainability index (γ_2) using R_v instead of R_t was also explored, i.e.:

$$\gamma_2 = (R_v \varphi (1-\eta))^{1/3} \tag{13}$$

2.5. Pairing of runoff replicates for impact assessment

To obtain the population of climate change impacts on the various reservoir characteristics, estimates of these characteristics for the current and corresponding future runoff are required. The best way to achieve the current-future runoff pairing is to use a 'two-site' stochastic generation approach (see McMahon and Adeloye, 2005), in which the current runoff is a 'site' and the future runoff is another 'site'. This approach was used by Peel et al. (2014) for quantifying the effect on runoff, etc. of climate change perturbations in the rainfall and temperature pair, considering each of these processes as a 'site'. However, multi-site data generation requires too much effort and can be problematic if the data are non-normally distributed. Consequently, a different approach which is much simpler to use was adopted in this study as follows.

After the stochastic generation of the required number of replicates (e.g. 1000 in the current case study) for the current and future runoff, a pair of integer numbers was randomly generated, with the 1st of these representing the current and the 2nd representing the future. This process was repeated until all the 1000 current and future runoff series have been paired up. If during the generation, a number is repeated (i.e. has been generated before), that pair is discarded and a new pair is generated. In this way the current and future hydrology scenarios (or runoff series) are paired up for the purpose of climate change impacts assessment. To accommodate the randomness in this approach, i.e. in which different pairing might result from repeated performance of the procedure, the exercise was repeated 100 times and the mean impact over the 100 repetitions was taken as the final impact due to climate change.

3. Case study

3.1. River basin and data

The Beas River, on which the Pong dam and its reservoir are located, is one of the five major rivers of the Indus basin in India (see Fig. 1). The reservoir drains a catchment area of 12,561 km^2, out of which the permanent snow catchment is 780 km^2 (Jain et al., 2007). Active storage capacity of the reservoir is 7290 Mm^3. Monsoon rainfall between July and September is a major source of water inflow into the reservoir, apart from snow and glacier melt. Snow and glacier melt runoff in Beas catchment was studied from 1990 to 2004 by Kumar et al. (2007) and its contribution is about 35% of the annual flow of the Beas River at Pandoh Dam (upstream of Pong dam). The reservoir meets irrigation water demands of 7913 Mm^3/year to irrigate 1.6 Mha of command area. The major crops cultivated in the area are rice, wheat and cotton. The seasonal distribution of the irrigation releases is shown in Fig. 4; these releases pass through hydropower turbines to generate electricity prior to being diverted to the irrigation fields. The installed capacity of hydropower plant is 396 kW. In general,

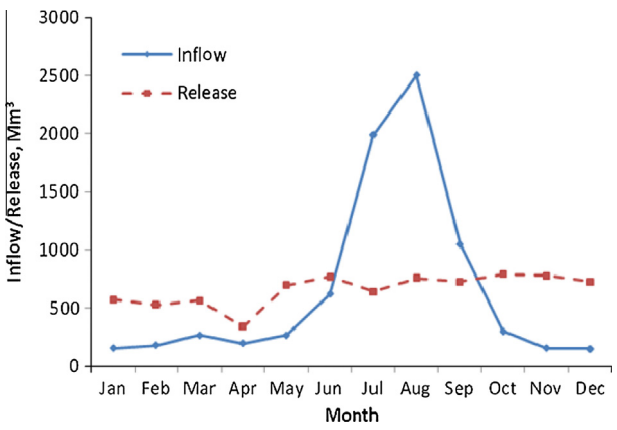

Fig. 4. Average monthly inflows and releases from Pong dam (2000–2008).

Fig. 4 reveals rises in release during the Kharif (June–October) cultivation season to cater for the water-intensive paddy rice cultivation during this season. Less water is released during the Rabi cultivation season (November–April); indeed, as Fig. 4 shows, the irrigation release is least in April at the end of the Rabi when only minor vegetables are cultivated.

Monthly reservoir inflow and release data from January 1998 to December 2008 (11 years) were available for the study. The historic mean annual runoff (MAR) at the dam site is 8485 Mm^3 (annual coefficient of variation is 0.225). The mean monthly flows are also shown in Fig. 4, which reveals the significantly higher inflows during the Monsoon season. In general, the irrigation demands are larger than the natural river flows except during the Monsoon, implying that such demands cannot be met without the Pong reservoir.

Gridded Tropical Rainfall Measuring Mission (TRRM 3B42 V7) daily rainfall data with the spatial resolution of 0.25° × 0.25° that span the runoff period were used. Potential evapotranspiration (ET_o) measurements were unavailable; hence they were obtained using the Penman–Monteith (P–M) formulation forced with meteorological variables from the NCEP Climate Forecast System Reanalysis (CFSR) data (spatial resolution = 0.5° × 0.5°) from January 1998 to December 2008. Because the spatial resolution of available rainfall and climatological data were different, the number of grids used to average rainfall, snowmelt and evapotranspiration were also different.

Although measured runoff data at the Pong dam were only available, to accommodate the spatial variability within the Beas catchment, the whole basin upstream of the dam was divided into three sub-basins: the upper, middle and lower as shown in Fig. 1, based on consideration of altitude, spatial difference, presence of hydraulic structures and available meteorological data. The sub-catchment areas are respectively 5720 km^2, 3440 km^2 and 3350 km^2. The Pandoh Dam is the hydraulic structure of note upstream of the Pong dam on the Beas and diverts water to the Sutlej River. Record of the diversion for the simulation period were obtained from the Bhakra-Beas Management Board (BBMB) and used to adjust the runoff reaching the Pong during the simulations.

HYSIM hydrological parameters were initialised with the help of the Harmonized World Soil Database (HWSD) analysis: the area of each soil type of the catchment was taken into account to get an average value of hydrological parameters. These parameters were then modified during the calibration of the model.

Finally, as noted in Section 2.4, the simulations for the performance evaluation require the operational rule curves for the Pong reservoir. In the absence of existing rule curves for the reservoir, genetic algorithms (GA) optimised rules curves (with integrated hedging) were developed as part of the wider study (see Adeloye et al., 2016), using the recorded historic runoff data at the Pong dam site. The basic form of these curves, i.e. without hedging, used in the current study is shown in Fig. 5.

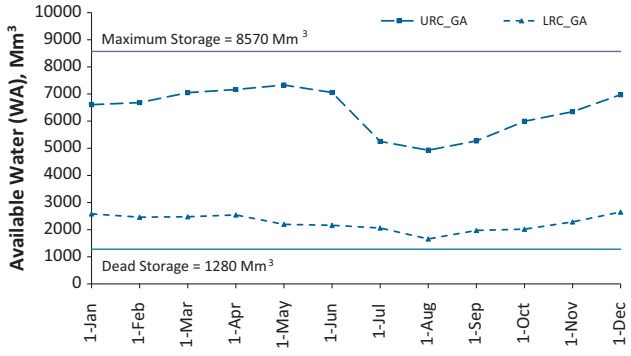

Fig. 5. GA optimised rule curves for the Pong reservoir.

3.2. Scenario neutral climate perturbations

Although scenario neutral perturbations of temperature (dT) and rainfall (dP) were used for the analyses, it is important that these perturbations are realistic. An objective way to ensure this is for the selected temperature and rainfall delta-perturbations to be guided by GCM projections of these climatic variables for the region of interest. Thus, we have examined the CMIP5 model simulations (Taylor et al., 2012; IPCC, 2013) for the Beas basin region to arrive at the temperature and rainfall perturbations used for the analyses.

Fig. 6 shows the scatter of the projected temperature and rainfall changes in the Beas Basin as obtained from 127 GCMs runs covering all CMIP5 representative concentration pathways (RCPs) for the short- (2011–2040), medium- (2041–2070) and the long-term (2071–2100) horizons. As seen in Fig. 6 all the GCMs are projecting temperature rise in the Beas with the projected change intensifying as the assumed radiative forcing intensifies and the

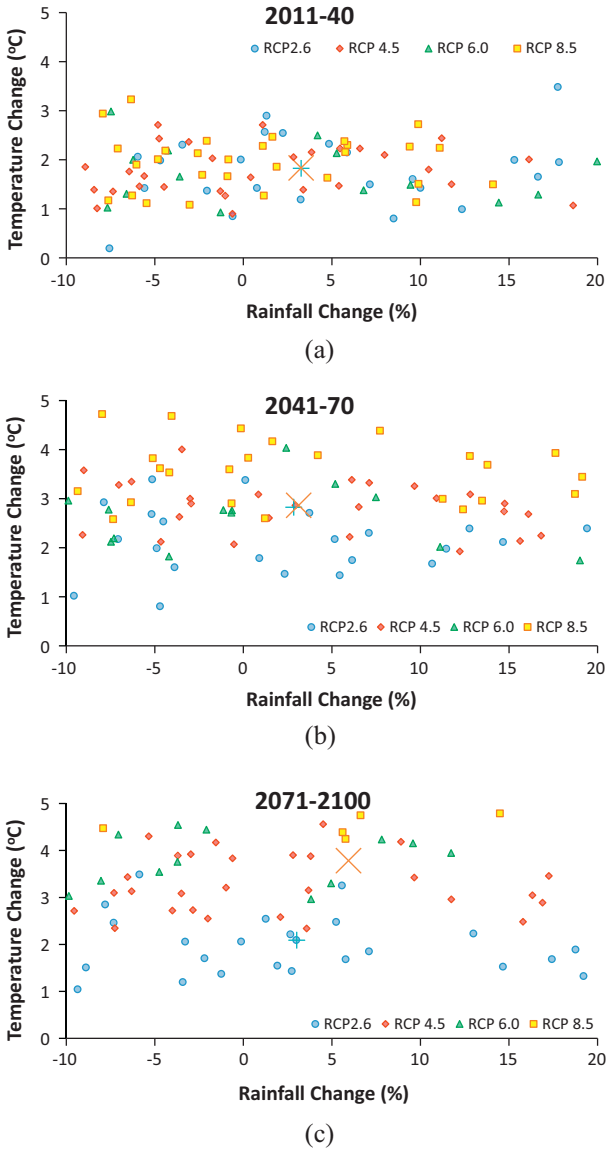

Fig. 6. Simulated changes in annual temperature and precipitation in the CMIP5-atlas ensemble relative to 1986–2005 (points show results of individual simulations; the crosses are the mean coordinates of the plotted points – see the text (Section 3.2) for further explanations).

time horizon lengthens. Indeed, majority of the projected changes for 2071–2100 horizon with RCP 8.5 were above 5 °C (which is why they have not been shown in the frame in Fig. 6c). Regarding rainfall, both reductions and increases in the annual rainfall are being projected by the GCMs. Unlike the temperature where there were noticeable differences between the RCPs, the projection in the annual rainfall was broadly similar, ranging from −10% to +20%.

One possibility for selecting the perturbations is to use ranges given by the 95% confidence limits of the mean co-ordinate of the data in Fig. 6. The mean co-ordinates of the scatter points are indicated by the crosses in Fig. 6. The 2041–2070 and 2071–2100 plots have two crosses because not all the projections have been shown on the frame. Thus, the lower cross represents the mean co-ordinate of the plotted points appearing on the frame while the higher cross is the mean co-ordinate if all the "out-of-range" values not shown on the frame are included. Obviously, given the large number of such out-of-range values in the 2071–2100 plots, the effect of including these has been more dramatic than in the 2041–2070 plot. These mean co-ordinates (or centroid of the changes) are summarised in Table 2, together with their corresponding 95% confidence limits, assuming that the means have a normal distribution.

As Table 2 shows, the 95% dT limits do capture the range of temperature changes projected by the GCMs; however, the same cannot be said about the dP limits which have completely omitted the reductions in rainfall projected by the models. Consequently, the climate change sensitivity analyses cannot be restricted to the limits shown in Table 2 but must involve the complete range as projected by the GCMs, especially in relation to projected reductions in rainfall because of its effect on reservoir inflows and hence on its performance. Following these considerations, delta perturbations in temperature (dT) of 0–5 °C (step of 1 °C) and annual rainfall perturbations (dP) of −10% to +20% (step of 5%) were finally used in the study. Although delta perturbations (or scenario-neutral) approach has often been criticised for its inability to accommodate future changes in the seasonality and probability distribution of climatic attributes and hence the runoff, it is nonetheless an efficient method in identifying tipping points at which a water resources infrastructure, e.g. a reservoir, is likely to fail catastrophically in meeting water demand.

4. Results and discussion

4.1. HYSIM rainfall–runoff model and assessed climate change impacts

The available flow record (1998–2008) was split into three: 1998–1999 (2 years) period was used for model warm-up, January 2000–December 2004 period was used for model calibration and January 2005–December 2008 period was used for model validation. The upper sub-catchment (see Fig. 1) of the Beas basin has permanent snow throughout the year. To simulate this permanent snow condition, we have added five years of data (January 1993–December 1997) to the upper sub-basin with the temperature fixed at zero (thus guaranteeing the availability of snow to be melted) and precipitation (in the form of snow) value of 15 mm on each day. This will add a permanent snow of ~27.4 m ($5 * 365 * 15$ mm) to the model. To accommodate model parameter uncertainty during calibration, a Monte Carlo approach involving the stochastic generation of hundred parameter sets for each sub-catchment during the calibration was used; the parameter set corresponding to the best-behaved simulation was finally selected.

As noted earlier, measured runoff data were only available for the outlet of the lower sub-catchment; consequently, comparison was only possible at this site. The performance of the model in simulating the runoff at the lower catchment outlet during calibration and validation is shown in Fig. 7a and b respectively. From these, it can be seen that the model has performed reasonably well in reproducing the measured runoff. More re-assuring is the relatively better performance of the model in simulating the low runoff sequence in the data, which is more important for water resources planning than the high flows periods. The estimated Nash–Sutcliffe efficiency indices during the calibration and validation were respectively 0.88 and 0.78, both of which lend further credence to the modelling skill of the calibrated HYSIM.

With HYSIM satisfactorily calibrated and validated, it was possible to use the validated model to assess impacts of changes in the rainfall and temperature on the runoff. As noted earlier, changes in annual rainfall considered were −10% to +20% with an increment of 5%. Similarly, temperature changes considered were 0 °C to +5 °C with an increment of unity. The mean values of the simulated annual and seasonal runoff are shown in Fig. 8. In general, reducing the rainfall causes the resulting runoff to reduce irrespective of the temperature situation. However, the simulation has also revealed a large influence of the melting glacier and seasonal snow on the runoff, where on an annual scale, changing the temperature by 2 °C is causing the runoff to increase by about a third. The simulations also reveal the dominance of the Monsoon effect on the runoff of the Pong. For example, of the simulated maximum mean annual runoff of about 12,000 Mm^3, almost 88% of this (~10,500 Mm^3) was contributed during the Monsoon (June to August) and post-monsoon (September to November) periods, with both the winter and pre-monsoon periods contributing the remaining 12%. This further reinforces the importance of the Monsoon in ensuring the water security of the Beas and indeed the whole of India.

Table 3 summarises the percentage change in annual and seasonal runoff relative to the simulated historic runoff. As expected, increasing the rainfall causes the annual runoff to increase while reducing the rainfall also causes the runoff to decrease for all the temperature scenarios. However, while increasing or decreasing the rainfall by the same amount has resulted in similar absolute change in the runoff for no change in temperature, the situation is quite different when temperature increases are also considered. For example, as shown in Table 3, an increase in annual rainfall of 5% produced a 10.21% increase in the annual runoff if the temperature increased by 1 °C; however, a similar decrease in rainfall with the 1 °C temperature increase only resulted in a decrease of only 1.6% in the annual runoff. As noted previously, the Beas hydrology is heavily influenced by the melting snow from the Himalayas and what these results show is that runoff contributed by the melting snow partially compensates for the reduction in direct runoff caused by the combined effects of lower rainfall and higher (temperature-induced) evapotranspiration. Indeed, as the assumed temperature increase becomes higher, the effect of any reduction in the annual rainfall fully disappears, resulting in a net increase in the annual runoff. Consequently, increasing the temperature by 2 °C has resulted in a net increase in the annual runoff of 12.4% and 7% for 5% and 10% reductions respectively in the annual rainfall.

Table 2
Mean and standard deviation of projected changes in temperature (dT) and annual rainfall (dP) based on 127 CMIP5 GCMs simulations.

Time slice	Mean (and standard deviation) of change		95% limits	
	dT (°C)	dP (%)	dT (°C)	dP (%)
2011–2040	1.84 (0.663)	2.84 (13.017)	[1.73, 1.96]	[0.58, 5.10]
2041–2070	2.94 (0.96)	2.77 (14.33)	[2.77, 3.11]	[0.28, 5.26]
2070–2100	3.90 (1.67)	5.51 (15.9)	[3.61, 4.19]	[2.74, 8.29]

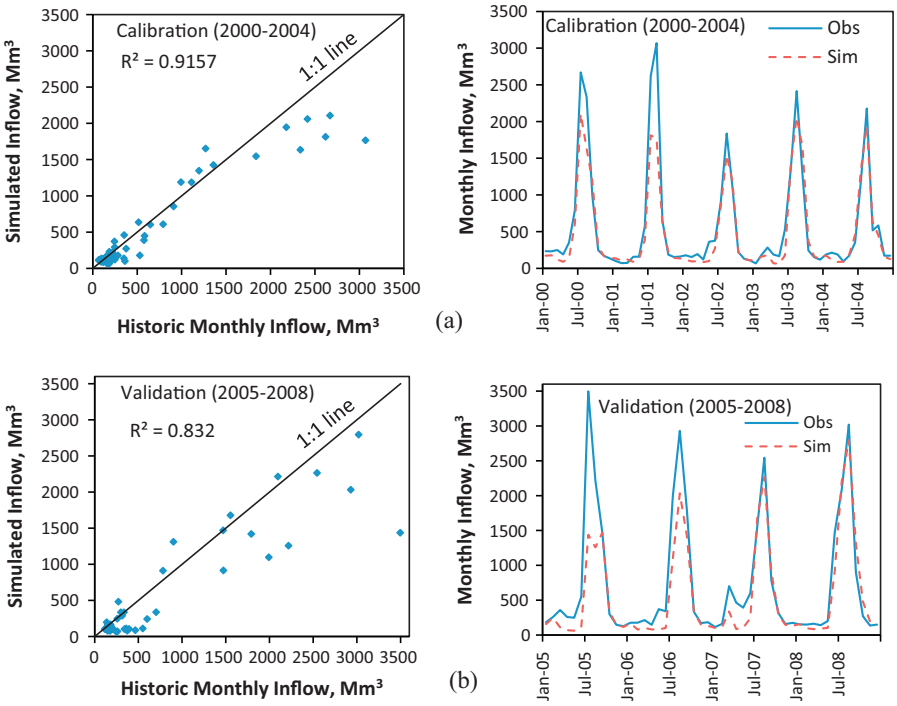

Fig. 7. Comparison of observed and simulated monthly river flow during: (a) calibration; and (b) validation.

The annual runoff situation presented above masks the significant seasonal differences in the simulated runoff response of the Beas. As Table 3 clearly shows, both the post-Monsoon and winter seasons that do not benefit from the melting snow and its associated runoff tended to be well-behaved in terms of the response, with reductions in the rainfall producing significant reductions in the generated runoff. Indeed, for these two seasons, increasing the temperature can worsen the runoff situation even for situations in which the rainfall has increased, as clearly revealed by the 2.4% reduction in the winter runoff with 1 °C and 5% rises, respectively in the temperature and rainfall. These situations must be resulting from the dominance of the evapotranspiration loss, which in the absence of additional water from melting snow will make the runoff to decrease.

4.2. Data generation

The skew of the untransformed (UT) monthly runoff data are shown in Table 4. Assuming that the skew has a normal distribution, then the approximate 95% confidence limits for zero skew is $[-1.96S_{gy}, 1.96S_{gy}]$ where S_{gy} is the standard error of estimate of the sample skew coefficient, given by $\sqrt{(6/n)}$, where n is the sample size. For $n = 11$, the 95% zero skew limits become [−1.45, 1.45], which means that statistically, the March runoff data cannot be assumed to be normally distributed. However, to avoid the use of mixed distributions, all the 12 months were subjected to the Box–Cox transformation as described in Section 2.2. The skew of the Box–Cox transformed data (Tr) are also shown in Table 4, together with the estimated transformation parameter (λ). As seen in Table 4, all the skew values for the transformed monthly runoff data are well within the 95% limits, implying that the transformed data exhibit the required near zero skew and can hence be described using the normal distribution.

The characteristics of the generated and simulated historic runoff (current) data are compared in Fig. 9. Similar results are available for the future runoff scenarios but these have been omitted here for lack of space. The generated statistics are the mean over the 1000 replicates. Fig. 9 shows the stochastic model has reasonably reproduced the mean, standard deviation and correlation of the simulated historic. The skewness is less well simulated, which is not surprising given that the skew was removed prior to the stochastic modelling. However, this should not be a major concern since reservoir capacity estimate is mostly influenced by the coefficient of variation, CV (i.e. standard deviation divided by the mean) and less by the skew (Burges and Linsley, 1971).

4.3. Uncertainty in capacity estimates

Population of reservoir capacity based on existing monthly irrigation releases at the Pong (see Fig. 1) are summarised in the box plots in Fig. 10a. The horizontal dashed line represents the existing (or historic) capacity of 7290 Mm^3. As Fig. 10a clearly shows, there is wide variability in the required reservoir capacity for each runoff scenario. Although the existing capacity of the Pong is 7290 Mm^3, the required capacity estimates based on the simulated current runoff series (see scenario T0_P0% in Fig. 10a) could be as low as 3545 Mm^3 or as high as 21,452 Mm^3. These, respectively, represent under-design and over-design situations relative to the existing capacity at the Pong reservoir. The implication of under design is that the reservoir will fail frequently to meet the demand.

The effect of climate change on the capacity estimates broadly follows the effect on runoff. Thus, as the rainfall and hence runoff decreases, the capacity required for meeting the demand increases. Consequently, a 5% decrease in the rainfall without a change in temperature (T0_P − 5%) would require a capacity as high as 21,540 Mm^3 to meet existing demands. However, when the rainfall increased by the same amount, (T0_P + 5%), the maximum capacity was 12,405 Mm^3. This is less than the maximum capacity for the T0_P0% scenario and may be caused by the fact that the additional rainfall especially in the already wet Monsoon season does not influence reservoir capacity estimate. When the rainfall changes are accompanied by increase in temperature, the resulting additional runoff has caused a reduction in the capacity requirement when compared to their corresponding no-temperature change situations.

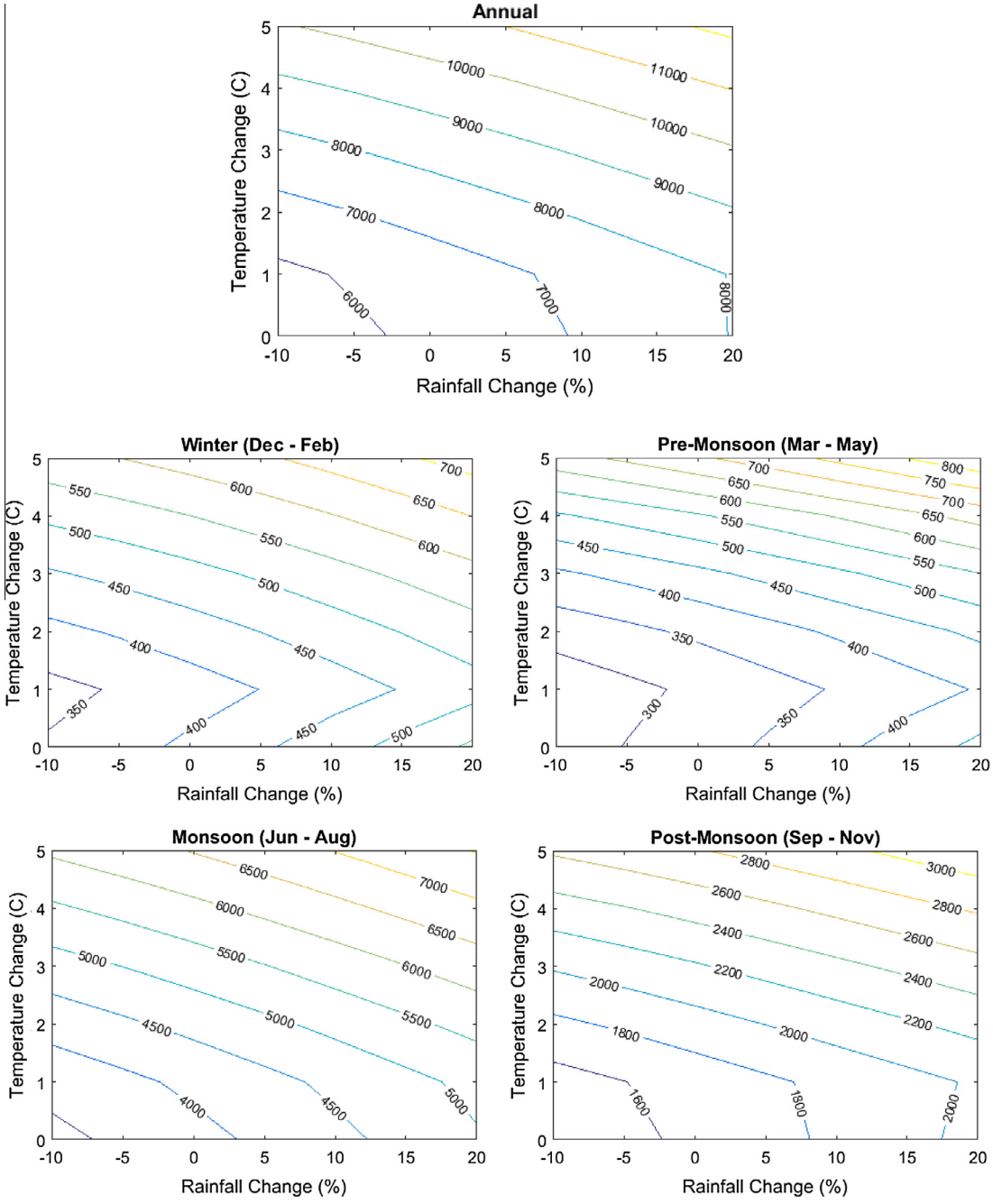

Fig. 8. Simulated mean annual and seasonal runoff at the Pong reservoir (Mm^3).

The variability or uncertainty of the reservoir capacity estimate is characterised by the coefficient of variation (CV) and summarised in Fig. 10d. This shows increasing uncertainty in required reservoir capacity as the catchment becomes drier. Kuria and Vogel (2015) recently presented the uncertainty (or CV) for water supply reservoir yields as a function of the inflow record length and the CV of annual runoff. Although the relationship between reservoir yield and capacity is non-linear, making it difficult to infer the variability in one from that of the other, the CV of the yield for the Beas record used (length = 11 years; CV = 0.225) if interpolated from Kuria and Vogel (2015) will be broadly within the CV envelope reported in Fig. 10d.

Fig. 10b summarises the population of changes in required reservoir capacity based on the paired experiments discussed earlier. As a reminder, the changes in Fig. 10b are the means over 100 replications of the paired experiments. Again, there are huge uncertainties in the predicted changes, which call into question the use of single runs of impact models in water resources climate change impact studies. Fig. 10b shows that the uncertainties are more pronounced for drier conditions than for wetter conditions. Thus, a 5% decrease in the rainfall can mean that the current capacity is either too little by as much as 195% or is too much by 47%. For the most wet future scenario investigated (T5_P + 20% – not shown in Fig. 10a to avoid cramping), the variability is much less, with the existing capacity representing an over design of between 42% and 63%.

The above large arrays of possibilities in the impact of climate change are bound to complicate decision making regarding adaptation and mitigation. Because impacts are not unique, it is obviously misleading to be talking of the impact because such does not exist.

Table 3
Change (%) of annual and seasonal runoff from simulated historic.

Temperature change, °C	Annual rainfall change, %						
	−10	−5	0	+5	+10	+15	+20
Annual							
0	−12.11	−6.25	0.00	6.70	13.77	21.26	29.22
1	−7.08	−1.63	4.17	10.21	16.44	22.80	29.28
2	6.98	12.41	18.19	24.27	30.51	36.90	43.40
3	22.89	28.33	34.12	40.21	46.52	52.97	59.57
4	40.44	45.94	51.78	57.93	64.32	70.87	77.52
5	59.50	65.01	70.86	77.03	83.46	90.04	96.75
Season: Winter (December–February)							
0	−13.25	−6.82	0.00	7.77	16.40	25.88	36.35
1	−18.32	−13.55	−8.19	−2.36	3.81	10.27	16.99
2	−5.90	−1.23	4.00	9.75	15.83	22.23	28.79
3	8.21	12.80	17.93	23.59	29.66	36.00	42.63
4	24.16	28.77	33.86	39.51	45.59	51.99	58.55
5	41.53	46.10	51.08	56.62	62.65	68.96	75.48
Season: Post-Monsoon (September–November)							
0	−10.80	−5.54	0.00	5.83	11.93	18.44	25.48
1	−7.60	−2.80	2.30	7.54	12.81	18.06	23.39
2	6.88	11.63	16.71	21.99	27.29	32.61	37.94
3	23.04	27.73	32.77	38.06	43.44	48.80	54.23
4	40.77	45.42	50.44	55.75	61.17	66.65	72.07
5	59.95	64.55	69.54	74.81	80.28	85.76	91.24
Season: Monsoon (June–August)							
0	−12.29	−6.35	0.00	6.76	13.85	21.26	29.01
1	−4.74	1.03	7.13	13.48	20.03	26.76	33.62
2	9.25	15.01	21.07	27.42	33.96	40.68	47.52
3	24.68	30.42	36.47	42.79	49.35	56.07	62.96
4	41.19	46.96	53.01	59.35	65.93	72.68	79.57
5	58.42	64.11	70.08	76.32	82.79	89.43	96.21
Season: Pre-Monsoon (March–May)							
0	−15.09	−7.92	0.00	8.89	18.82	29.65	41.46
1	−17.76	−12.05	−5.72	1.09	8.29	15.72	23.37
2	−2.96	3.03	9.70	16.94	24.58	32.56	40.69
3	19.57	26.28	33.62	41.61	50.04	58.77	67.79
4	50.53	58.17	66.41	75.27	84.64	94.46	104.50
5	92.34	101.57	111.41	122.07	133.34	145.14	157.29

Table 4
Box–Cox transformation parameter (λ) and the skew coefficient for untransformed (UT) and transformed (Tr) monthly flow values for current runoff scenario.

	January	February	March	April	May	June	July	August	September	October	November	December
UT	−0.35	1.15	1.97	−0.89	0.80	0.99	0.05	0.49	−0.38	0.38	1.03	0.87
Tr	−0.22	0.12	0.33	−0.33	0.01	0.0	−0.07	0.0	−0.22	0.0	0.01	0.0
λ	2.16	−1.05	−1.93	0.90	−0.16	−0.02	0.75	0.06	1.44	−0.03	−2.21	−1.40

However, what can be done is to attach likelihood (or probability) of occurrence to the assessed impacts. Fig. 10c shows the empirical cumulative distribution function (CDF) of required capacity estimates for all the investigated scenarios and reveals the rightward shift in the CDF as the catchment becomes drier, implying higher storage requirements at a given probability. Additionally, not only are the drier conditions requiring more storage at a given probability, their CDFs are also less steep resulting in significant differences between the lower and higher quantiles of the capacity estimates.

4.4. Uncertainty in reservoir performance

The Box plots for the performance indices are shown in Fig. 11a–e. In order to save space, however, the Box plots of the changes in these indices as well as their empirical CDFs are not reproduced here but can be requested from the corresponding author by interested readers.

The two reliability indices, R_v and R_t, shown in Fig. 11a and b respectively also exhibit variability in their estimates, however, a quick juxtaposition of both figures will reveal that $R_t < R_v$ as expected, which is why caution should be exercised when adopting the time-based reliability for system evaluation: the fact that time-based reliability is low does not make the water supply situation of the system poor. Thus, as noted by Adeloye (2012), while the initial evaluation of systems performance can be based on the time based reliability R_t because it is simple to estimate and might be readily recognised by users who are already familiar with the concept of return periods, the volumetric reliability should also be evaluated and any necessary adjustments made to system's characteristics in the light of this. For example, the R_t may be relaxed (or reduced), such as through increasing the release from the reservoir to meet additional needs or adopting a lower reservoir capacity during planning, if the R_v is very high. From Fig. 11b, it is evident that, R_t is improving when the rainfall is increasing as expected; similarly temperature increases also improved the R_t, due to additional runoff availability from snow and glacier melt from the Himalayas. Contrary to R_t, the R_v shows less variability for all the scenarios.

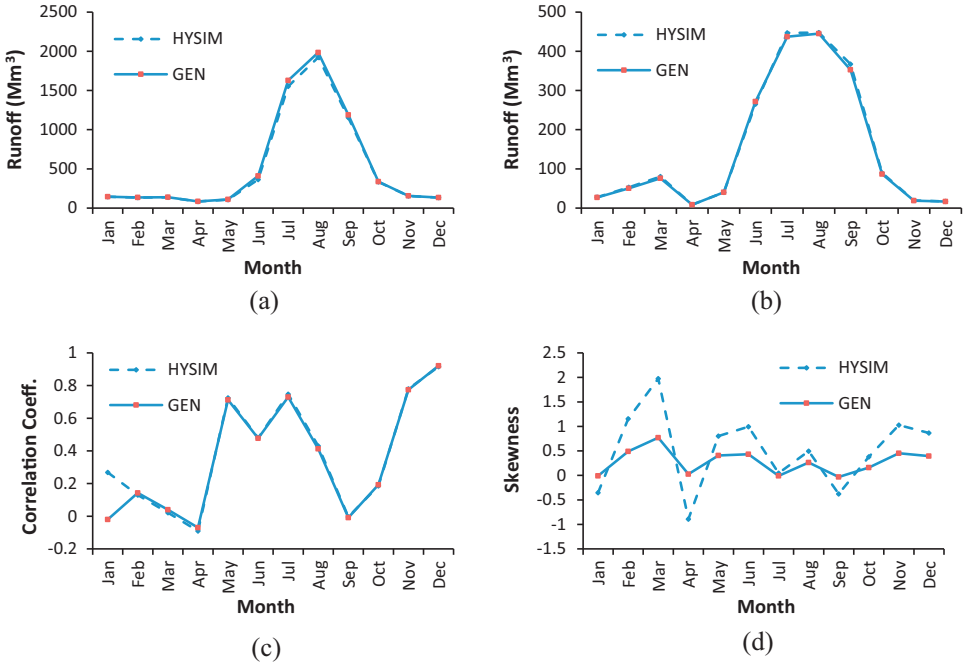

Fig. 9. Comparison of statistics of 'observed' (HYSIM) and stochastically generated (GEN) runoff: (a) mean; (b) standard deviation; (c) correlation coefficient; and (d) skewness.

Fig. 11c shows the resilience (i.e. probability of recovering from failure) and reveals that, increasing the rainfall also improves the resilience. The population of the assessed vulnerability is summarised in Fig. 11d and shows that in general, the mean vulnerability is decreasing when the rainfall and temperature are increasing, i.e. when the inflow is increasing, as expected but this is at the expense of an expanding variability or uncertainty. For example, although the assessed vulnerability of the Pong reservoir is about 66% based on single run of the historic runoff record, the vulnerability for this T0_P0 situation could actually be either as low as 56% or as high as 97% if the stochastic properties of the historic runoff are taken into account. In general, vulnerability (or single period deficits) above 25% is not recommended because of the distress it can cause to water users (Fiering, 1982). Thus, the fact that the least historic vulnerability obtained for the Pong reservoir exceeds 25% is an indication that changes in existing operational practices, e.g. by hedging, conjunctive use with other sources such as groundwater, etc., are required to temper the large single period shortage. As the inflow increases, the lower range of the vulnerability drops, sometimes approaching zero but its upper range also rises, making the estimate of the vulnerability more uncertain.

The sustainability index γ is a figure of merit that integrates the three basic performance indices of reservoir performance – reliability, resilience and vulnerability – thus making it possible to avoid the complexities that can arise in using multi-criteria (and their possible trade-offs as explained earlier in the case of R_t and R_v) in decision making. The population of γ is shown in Fig. 11e which also reveals high variability as would be expected from the behaviour of its constituent indices. The variation with respect to the historic sustainability of 0.44 appears much larger for the drier scenarios than the wetter scenarios, thus resembling the behaviour of the resilience (see Fig. 11c). Although the form of the sustainability index adopted in this work (see Eq. (12)) is meant to temper the dominating effect (including the so-called "nullity" problem where if any of the constituent indices is zero, the γ is also zero – see Chiamsathit et al. (2014)) of any of the constituent indices over the other, it would seem that the resilience, being the smallest numerically of all the constituent indices of the sustainability (γ), is still exerting a strong influence on the γ. Although not shown in Fig. 11 to save space, the use of R_v (as opposed to R_t) in γ (see Eq. (13)) did not result in any significant change in the population of the γ. This may be largely due to the fact that the estimated γ is more affected by the resilience and less by the reliability (time- and volume-based) as explained earlier.

The variability (or CV) of the assessed performance indices are summarised in Fig. 12a–f and confirm the observation made earlier from considerations of the Box plots. Of the performance indices, the two reliability measures, R_t and R_v, were the least variable with the R_v being the more reliable of the two (see Fig. 12a and b). Furthermore, the trend in the two reliability measures was similar to that of the reservoir capacity in that their variability increased as the catchment became drier. Although the relative popularity of these two indices for reservoir performance evaluation has often been attributed to their ease of estimation, the fact that they also exhibit the least variability should further entrench their usefulness for reservoir planning analysis.

The vulnerability was the most variable (see Fig. 12d), with the CV exceeding 50% for very wet catchment conditions as would be expected from the expanding range in its population as noted earlier. The vulnerability is a useful index for assessing the impact of water shortage on users; however, what this study has shown is that its estimate can be highly variable, which calls for caution in its use. For relatively drier situations when the possibility of water shortage is more likely, the variability of the vulnerability is much lower, thus making its use for decision making in such difficult situations less problematic.

The variability in the sustainability index (see Fig. 12e and f) was much tempered when compared to the variability in the vulnerability, whereas there is broad variability resemblance between the sustainability and resilience (see Fig. 12c). Both the resilience and sustainability also exhibit similar trend in the variability, i.e. the variability in the two indices appears to increase as the catchment becomes wetter, which may further help to explain why the resilience is such a dominant index

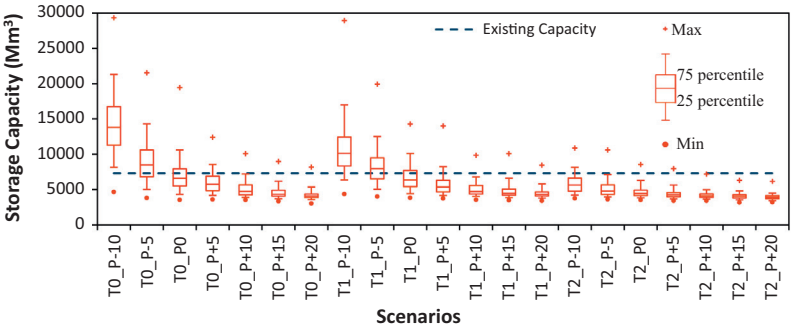

(a)

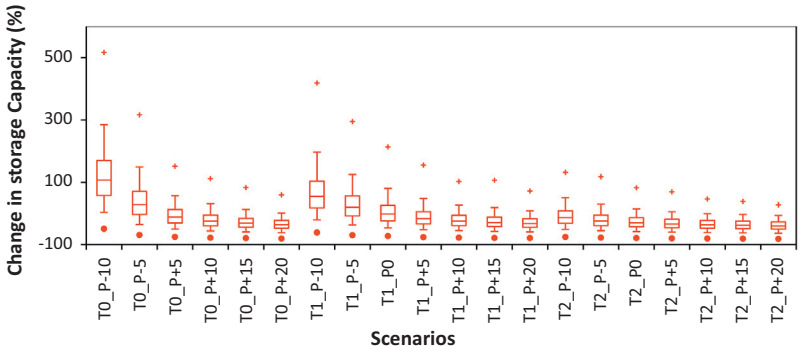

(b)

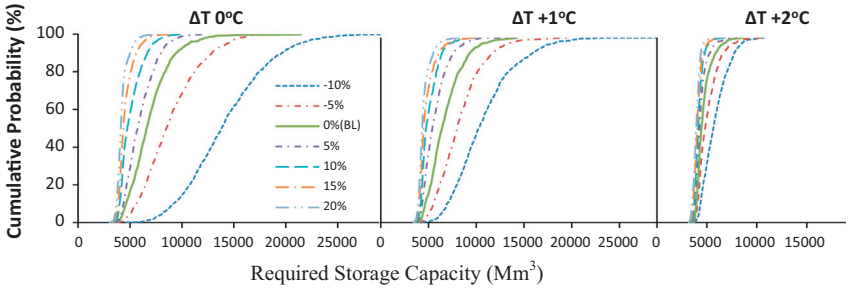

(c)

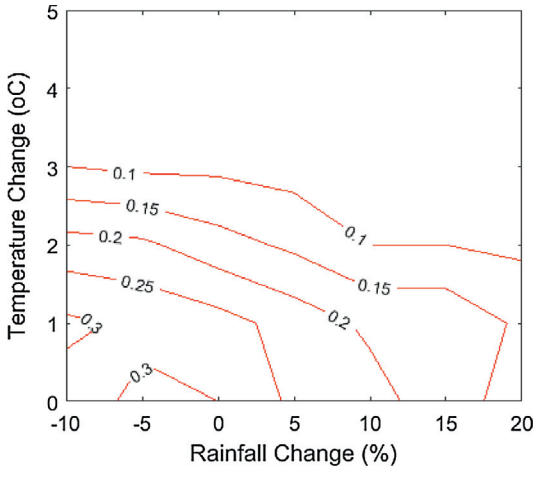

(d)

Fig. 10. Reservoir storage: (a) box plot of required storage capacity; (b) change (%) in required storage capacity; (c) CDF of required storage capacity; (d) CV of required storage capacity.

on the estimated sustainability as observed previously. The use of R_v instead of R_t in the sustainability index (compare Fig. 12e and f) did not produce any noticeable effect on the variability of the sustainability, which is not surprising given the low and broadly similar variabilities of the two reliability measures (as seen in Fig. 12a and b).

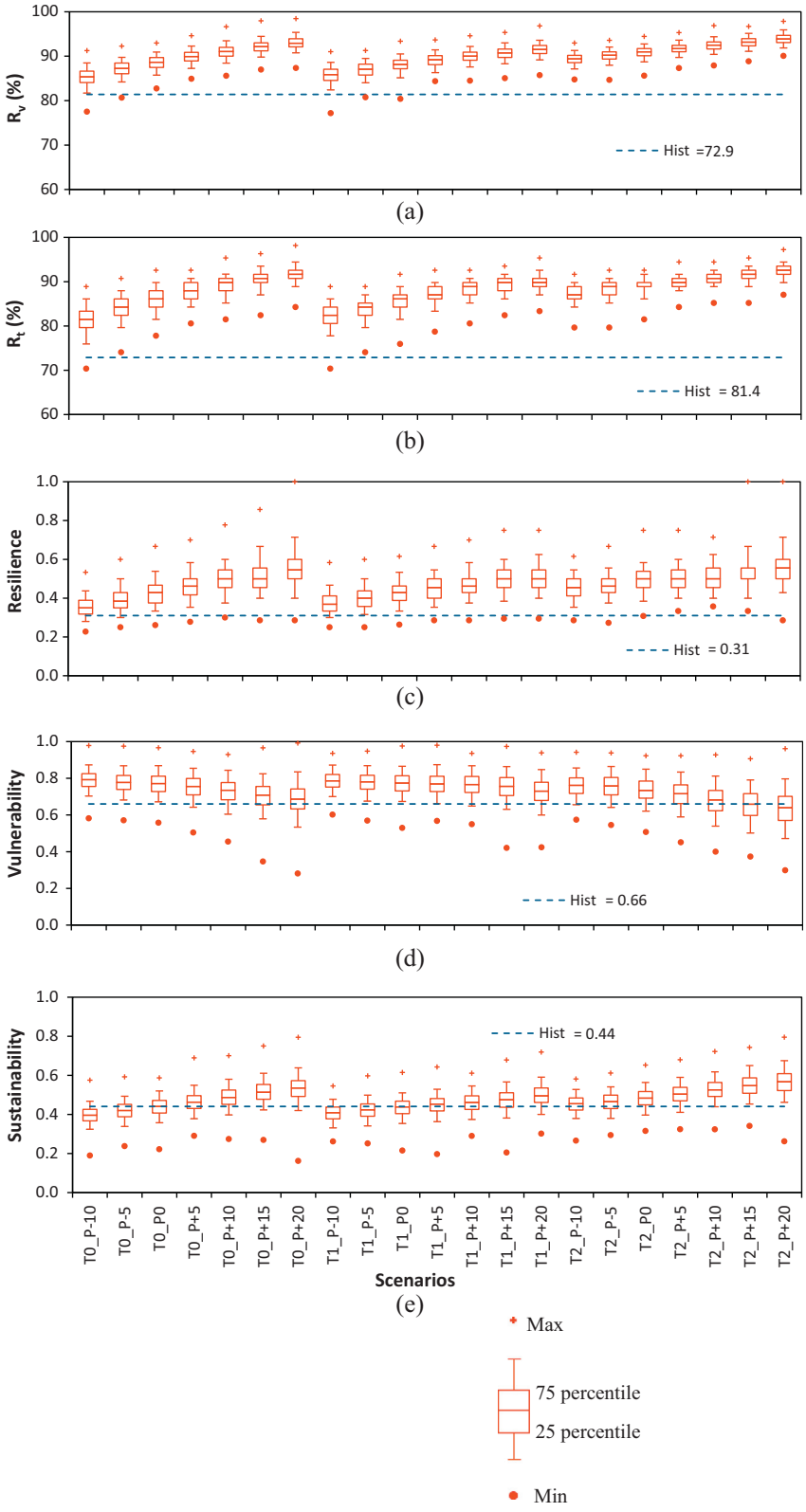

Fig. 11. box plot of reservoir performance: (a) volume reliability; (b) time reliability; (c) resilience; (d) vulnerability; (e) sustainability (based on R_t).

The above clearly offers useful insights into the use of the performance indices for reservoir assessment. On the basis of the variability, the two reliability measures (R_v and R_t) remain the best but given that R_v actually quantifies the volume of water supplied and is the least variable, R_v should be preferred. The high variability in both the vulnerability and resilience makes them unreliable for decision making but the sustainability index which integrates these with all other indices is less variable and should form the avenue for accommodating both the vulnerability and resilience in performance evaluation.

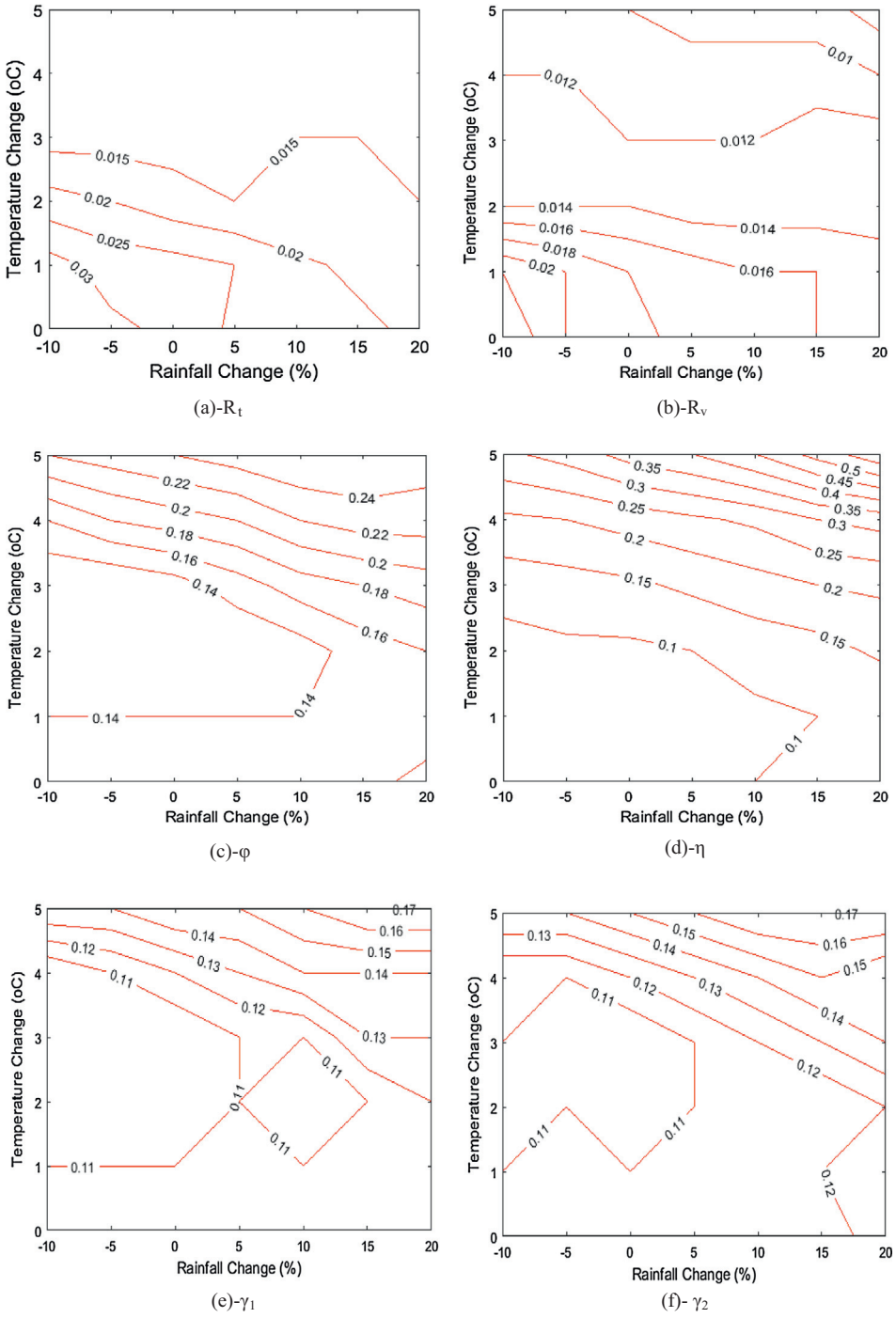

Fig. 12. CV of performance indices: (a) time reliability; (b) volume reliability; (c) resilience; (d) vulnerability; (e) sustainability (based on R_t); (f) sustainability (based on R_v).

5. Conclusions

This study has revealed the large variability associated with climate change impacts assessment and the importance of characterising this variability for improved decision making. The application of the methodology to the Pong reservoir on the Beas River in norther India used delta perturbations in both the rainfall and temperature that were informed by CMIP5 GCM simulations. As expected, reductions in rainfall resulted in reservoir inflow runoff to decrease and vice versa. However, due to the effect of melting snow and glaciers that are abundant within the Beas catchment, increasing temperature and the resulting melting of the snow and glacier nullified some of the impacts of reduced rainfall on the inflow.

As far as the planning characteristics of the Pong reservoir were concerned, the reservoir capacity needed to maintain existing levels of irrigation water releases from the reservoir was highly variable in comparison to the existing capacity at the dam. In particular, it has been revealed that the needed capacity for future conditions may either be as much as 83% lower or 506% higher depending on the climate scenario. Both of these situations are undesirable due to capital lock-in in the case of the latter and systems poor performance for the former. The derived empirical distribution of the reservoir capacity showed rightward shifting and

less steep CDFs as the catchment became drier, implying that that reservoir capacity quantiles for drier scenarios are much larger than the corresponding values for wetter conditions.

The associated reservoir performance indices are also variable. Of these, the vulnerability exhibited the highest variability which in the worst case was as high 50%. The two reliability indices, R_t and R_v, were the least variable, with the R_v exhibiting slightly lower CVs than the R_t. This further underscores the popularity of the two indices for water resources systems evaluation.

The outcome of the study has clearly exposed the dangers of mean climate impacts assessments which fail to characterise the variability of the assessed impacts. It should certainly be desirous for decision makers to have full picture of the likely range of impacts to be expected and the risks (or probabilities) of occurrence of such impacts so that effective adaptation measures, e.g. improved reservoir operational practices involving water hedging that deliberately withholds water during normal operation for later release when conditions are drier, conjunctive use of groundwater and surface water resources, etc. can be developed and appropriately prioritised. The methodology reported in this work will provide answers to these questions, is simple to implement and, although applied to one system, can readily be replicated for other water resources systems. It is also the only study as far as we are aware that has extended the characterisation of uncertainties to reservoir performance indices.

Acknowledgements

The work reported here was funded by the UK-NERC (Project NE/I022337/1) – Mitigating Climate Change impacts on India Agriculture through Improved Irrigation Water Management (MICCI) – as part of the UK-India Changing Water Cycle (CWC South Asia) thematic Programme.

References

Adeloye, A.J., 2012. Hydrological sizing of water supply reservoirs. In: Bengtsson, L., Herschy, R.W., Fairbridge, R.W. (Eds.), Encyclopedia of Lakes and Reservoirs. Springer, Dordrecht, pp. 346–355.

Adeloye, A.J., Montaseri, M., Garman, C., 2001. Curing the misbehaviour of reservoir capacity statistics by controlling shortfall during failures using the modified sequent peak algorithm. Water Resour. Res. 37 (1), 73–82.

Adeloye, A.J., Nawaz, N.R., Bellerby, T.J., 2013. Modelling the impact of climate change on water systems and implications for decision makers. In: Surampali, R.Y., Zhang, T.C., Ojha, C.S.P., Gujar, B.R., Tyagi, R.D., Kao, C.M. (Eds.), Climate Change Modelling, Mitigation, and Adaptation. Environmental & Water Resources Institute, American Society of Civil Engineers (ASCE), USA, pp. 299–326, ISBN: 978078441271 (Chapter 11).

Adeloye, A.J., Soundharajan, B., Ojha, C.S.P., Remesan, R., 2016. Effect of hedging integrated rule curves on the performance of the Pong Reservoir (India) during scenario-neutral climate change perturbations. Water Resour. Manage. 30 (2), 445–470. http://dx.doi.org/10.1007/s11269-015-1171-z.

Anandhi, A., Frei, A., Pierson, D.C., Schneiderman, E.M., Zion, M.S., Lounsbury, D., Matonse, A.H., 2011. Examination of change factor methodologies for climate change impact assessment. Water Resour. Res. 47.

Arnell, N.W., 2003. Relative effects of multi-decadal climatic variability and changes in the mean and variability of climate due to global warming: future stream flows in Britain. J. Hydrol. 270, 195–213.

Burges, S.J., Linsley, R.K., 1971. Some factors influencing required reservoir storage. J. Hydraul. Div. ASCE 97 (7), 977–991.

Burn, H.D., Simonovic, S.P., 1996. Sensitivity of reservoir operation performance to climatic change. Water Resour. Manage. 10 (6), 463–478.

Chiamsathit, C., Adeloye, A.J., Soundharajan, B., 2014. Assessing competing policies at Ubonratana reservoir, Thailand. Proc. ICE-Water Manage. 167 (10), 551–560.

Fiering, M.B., 1982. Estimates of resilience indices by simulation. Water Resour. Res. 18 (1), 41–50.

Fowler, H.J., Blenkinsop, S., Tebaldi, C., 2007. Linking climate change modelling to impacts studies: recent advances in downscaling techniques for hydrological modelling. Int. J. Climatol. 27 (12), 1547–1578.

Fowler, H.J., Kilsby, C.G., O'Connell, P.E., 2003. Modeling the impacts of climatic change and variability on the reliability, resilience and vulnerability of a water resource system. Water Resour. Res. 39 (8).

Hashimoto, T., Stedinger, J.R., Loucks, D.P., 1982. Reliability, resilience and vulnerability criteria for water resources system performance evaluation. Water Resour. Res. 18 (1), 14–20.

IPCC, 2007. Summary for Policymakers. Climate Change 2007: The Physical Science Basis, Contribution of the Working Group I to the Fourth Assessment Report of the Intergovernmental Panel on Climate Change. Cambridge University Press.

IPCC, 2013. Annex I: atlas of global and regional climate projections [van Oldenborgh, G.J., Collins, M., Arblaster, J., Christensen, J.H., Marotzke, J., Power, S.B., Rummukainen, M., Zhou, T. (Eds.)]. In: Stocker, T.F., Qin, D., Plattner, G.-K., Tignor, M., Allen, S.K., Boschung, J., Nauels, A., Xia, Y., Bex, V., Midgley, P.M. (Eds.), Climate Change 2013: The Physical Science Basis. Contribution of Working Group I to the Fifth Assessment Report of the Intergovernmental Panel on Climate Change. Cambridge University Press, Cambridge, United Kingdom and New York, NY, USA.

Jain, S.K., Agarwal, P.K., Singh, V.P., 2007. Hydrology and Water Resources of India. Springer, The Netherlands.

Kumar, V., Singh, P., Singh, V., 2007. Snow and glacier melt contribution in the Beas River at Pandoh Dam, Himachal Pradesh, India. Hydrol. Sci. J. 52 (2), 376–388.

Kuria, F., Vogel, R., 2015. Uncertainty analysis for water supply reservoir yields. J. Hydrol. 529 (1), 257–264.

Li, L., Xu, H., Chen, X., 2009. Streamflow forecast and reservoir operation performance assessment under climate change. Water Resour. Manage. 24, 83–104.

Lopez, A., Fung, F., New, M., 2009. From climate model ensembles to climate change impacts and adaptation: a case study of water resource management in the southwest of England. Water Resour. Res. 45, W08419.

Manley, R.E.Water Resources Associates (WRA), 2006. A Guide to Using HYSIM (Version 4.90). R.E. Manley and Water Resources Associates Ltd., Wallingford, UK.

McMahon, T.A., Adeloye, A.J., 2005. Water Resources Yield. Water Resources Publications, Littleton, CO, USA.

McMahon, T.A., Adeloye, A.J., Zhou, S.L., 2006. Understanding performance measures of reservoirs. J. Hydrol. 324, 359–382.

McMahon, T.A., Mein, R.G., 1986. River and Reservoir Yield. Water Resources Publ., Col., USA.

Murphy, C., Fealy, R., Charlton, R., Sweeney, J.S., 2006. The reliability of an "off the shelf" conceptual rainfall–runoff model for use in climate impact assessment: uncertainty quantification using Latin Hypercube Sampling. Area 38 (1), 65–78.

Nawaz, N.R., Adeloye, A.J., 2006. Monte Carlo assessment of sampling uncertainty of climate change impacts on water resources yield in Yorkshire, England. Clim. Change 78, 257–292.

Peel, M.C., Srikanthan, R., McMahon, T.A., Karoly, D.J., 2014. Uncertainty in runoff based on global climate model precipitation and temperature data – part 2: estimation and uncertainty of annual runoff and reservoir yield. Hydrol. Earth Syst. Sci. 11, 4579–4638.

Pilling, C., Jones, J.A.A., 1999. High resolution climate change scenarios: implications for British runoff. Hydrol. Process. 13 (17), 2877–2895.

Pilling, C.G., Jones, J.A.A., 2002. The impact of future climate change on seasonal discharge, hydrological processes and extreme flows in the Upper Wye experimental catchment, Mid-Wales. Hydrol. Process. 16, 1201–1213.

Pretto, P.B., Chiew, F.H.S., McMahon, T.A., Vogel, R.M., Stedinger, J.R., 1997. The (mis) behavior of behavior analysis storage estimates. Water Resour. Res. 33 (4), 703–709.

Raje, D., Mujumdar, P.P., 2010. Reservoir performance under uncertainty in hydrologic impacts of climate change. Adv. Water Resour. 33, 312–326.

Ripple, W., 1883. Capacity of storage reservoirs for water supply. Minut. Proc., Inst. Civ. Eng. 71, 270–278.

Sandoval-Soils, S., Mckinney, D.C., Loucks, D.P., 2011. Sustainability index for water resources planning and management. J. Water Resour. Plan. Manage. (ASCE) 137 (5), 381–389.

Savic, D.A., Burn, D.H., Zrinji, Z., 1989. A comparison of streamflow generation models for reservoir capacity-yield analysis. Water Resour. Bull. 25 (5), 977–983.

Silva, A.T., Portela, N.M., 2012. Stochastic assessment of reservoir storage-yield relationships in Portugal. J. Hydrol. Eng., ASCE 18 (5), 567–575.

Srikanthan, R., McMahon, T.A., 1982. Stochastic generation of monthly streamflows. J. Hydraul. Div., ASCE 108 (HY3), 419–441.

Svanidze, G.G., 1964. Osnovy rascheta regulirovaniya rechnogo stoka metodom Monte-Karlo (Elements of River Runoff Regulation Computation by Monte Carlo Method). Tbilivi Izdatel'stro Metsmiereba.

Taylor, K.E., Stouffer, R.J., Meehl, G.A., 2012. An overview of CMIP5 and the experiment design. Bull. Am. Meteor. Soc. 93, 485–498.

Thomas, H.A., Fiering, M.B., 1962. Mathematical synthesis of streamflow sequence for the analysis of river basins simulations. In: Maass, A. et al. (Eds.), Design of Water Resources Systems. Harvard University.

Valencia, D., Schaake, J.C., 1973. Disaggregation process in stochastic hydrology. Water Resour. Res. 9 (3), 580–585.

Vicuna, S., McPhee, J., Garreaud, R.D., 2012. Agriculture vulnerability to climate change in a snowmelt-driven basin in semiarid Chile. J. Water Resour. Plan. Manage., ASCE 138 (5), 431–441.

Wilby, R.L., 2005. Uncertainty in water resource model parameters used for climate change impact assessment. Hydrol. Process. 19 (16), 3201–3219.